

3D ANATOMICAL STRUCTURE-GUIDED DEEP LEARNING FOR ACCURATE DIFFUSION MICROSTRUCTURE IMAGING

Xinrui Ma^{1,2}, Jian Cheng^{3,4}, Wenxin Fan^{1,2}, Ruoyou Wu^{1,2,5}, Yongquan Ye⁶, Shanshan Wang^{1,†}

¹Paul C. Lauterbur Research Center for Biomedical Imaging, Shenzhen Institutes of Advanced Technology, Chinese Academy of Sciences, Shenzhen, Guangdong, China

²University of Chinese Academy of Sciences, Beijing, China

³State Key Laboratory of Software Development Environment, Beihang University, Beijing, China.

⁴Key Laboratory of Data Science and Intelligent Computing, Institute of International Innovation, Beihang University, Hangzhou, Zhejiang, China

⁵Pengcheng Laboratory, Shenzhen, Guangdong, China

⁶United Imaging Healthcare, Houston, TX, USA

ABSTRACT

Diffusion magnetic resonance imaging (dMRI) is a crucial non-invasive technique for exploring the microstructure of the living human brain. Traditional hand-crafted and model-based tissue microstructure reconstruction methods often require extensive diffusion gradient sampling, which can be time-consuming and limits the clinical applicability of tissue microstructure information. Recent advances in deep learning have shown promise in microstructure estimation; however, accurately estimating tissue microstructure from clinically feasible dMRI scans remains challenging without appropriate constraints. This paper introduces a novel framework that achieves high-fidelity and rapid diffusion microstructure imaging by simultaneously leveraging anatomical information from macro-level priors and mutual information across parameters. This approach enhances time efficiency while maintaining accuracy in microstructure estimation. Experimental results demonstrate that our method outperforms four state-of-the-art techniques, achieving a peak signal-to-noise ratio (PSNR) of 30.51 ± 0.58 and a structural similarity index measure (SSIM) of 0.97 ± 0.004 in estimating parametric maps of multiple diffusion models. Notably, our method achieves a $15\times$ acceleration compared to the dense sampling approach, which typically utilizes 270 diffusion gradients.

Index Terms— deep learning, diffusion MRI, microstructural estimation, multiple diffusion models

1. INTRODUCTION

Diffusion magnetic resonance imaging (dMRI) is widely applied to non-invasively estimate brain tissue microstructure by measuring the restricted diffusion of water molecules in the local microstructural environment. By carefully designing signal models that relate tissue microstructure to diffusion signals, the organization of the neuronal tissue can be inferred by fitting these models to the observed measurements. For example, diffusion tensor imaging (DTI) [1] is a classic signal model that assumes Gaussian diffusion of water molecules in voxels. Although DTI is a commonly used signal model, it is known to lack specificity [2]. To improve the specificity of dMRI

in quantifying tissue complexity and heterogeneity, advanced diffusion models like neurite orientation dispersion and density imaging (NODDI) [3] have been developed. Notably, rotationally invariant scalar measures from NODDI have been widely used in neuroscientific research. However, fitting the NODDI model currently requires a large number of diffusion gradients (about 100 or more), resulting in a long acquisition time (approximately half an hour for 270 gradients) [2, 4]. Clinical scan time for dMRI is often limited to a few minutes, typically allowing for only about 30 diffusion gradients or fewer [2]. Moreover, dMRI scans have the problems of low signal-to-noise ratio (SNR) and reproducibility [5]. Recently deep learning (DL) techniques have been applied to accelerate diffusion MRI, yielding promising results [6]. The seminal work of Golkov et al. [7] introduced the deep learning concept to diffusion MRI and established the q-space deep learning (q-DL) framework, which has greatly benefited the subsequent work in this field. q-DL and subsequent studies have also demonstrated the promise of deep learning in using a small amount of diffusion data to predict high-quality scalar diffusion metrics from DTI [8, 9, 10] and more advanced diffusion analysis models, such as NODDI [7, 11, 12, 13].

To better understand brain microstructure, integrating features from multiple diffusion models is clinically beneficial, though it increases the demands of model fitting and computational cost. To tackle these challenges, HashemizadehKolowri et al. [14] compared three different DL approaches proposed to jointly estimate parametric maps of DTI, diffusion kurtosis imaging (DKI), NODDI, and multi-compartment spherical mean technique (SMT). Fan et al. [15] proposed DeepMpmMRI, equipped with a newly designed tensor-decomposition-based regularizer, for simultaneously estimating parametric maps of DTI and NODDI. Li et al. [4] reconstructed tissue microstructure from four brain dMRI datasets using the NODDI and SMT models, providing evidence for the clinical feasibility of DL-based tissue microstructure reconstruction.

Integrating anatomical priors with diffusion images is essential for enhancing the directionality and accuracy of diffusion signal interpretations [16, 17]. Chen et al. [18] proposed DCS-qL, a model that incorporates multiple network branches to process patches with distinct tissue labels, thereby enhancing tissue-specific representation and diffusion signal interpretation. Huang et al. [19] proposed a novel method, namely PAK-SRR, to employ rich prior anatomical knowledge (PAK) as strong guidance to improve the super reso-

[†] Corresponding author: ss.wang@siat.ac.cn

lution reconstruction of fetal brain MRI. Li et al. [20] introduced DeepAnat to synthesize high-quality T1-weighted(T1w) anatomical images directly from diffusion data, enabling brain segmentation and facilitating co-registration in scenarios where T1w images are unavailable. Inspired by these pioneering works, we consider key anatomical priors based on tissue probability maps to guide microstructure estimation from multiple diffusion models.

To this end, we propose a deep learning-based framework for brain microstructure estimation that incorporates rich prior anatomical knowledge as an additional regularization term. This framework aims to simultaneously estimate parameters derived from diverse diffusion models using sparsely sampled q-space data. First, we utilize anatomical priors from three tissue probability maps obtained from T1w images. By aligning diffusion signals with anatomical boundaries, this approach effectively mitigates inaccuracies in parameter estimation that can arise from blurry tissue boundaries in the brain. Second, we have developed a highly extensible framework capable of accommodating various diffusion models. This framework employs a flexible network architecture as its backbone, enabling the leveraging of mutual information across parameters to enhance overall accuracy.

2. METHOD

2.1. Task Formulation

By applying a set of diffusion gradients, we can acquire a vector of diffusion signals at each voxel. Each diffusion signal can be considered as a set of $W \times H \times S$ size volumes captured in the q-space. Thus the dMRI data are 4D signals of size $\mathbb{R}^{W \times H \times S \times D}$, where W, H, S, D refer to the width, height, slice, and gradient directions, respectively. We aim to estimate the multiple parameters derived from various diffusion models using sparsely sampled q-space data. Given the diffusion MRI data $\mathcal{X} \in \mathbb{R}^{W \times H \times S \times D_{Full}}$, containing the full measurements in the q-space, we can obtain the corresponding ground-truth scalar maps \mathcal{Y}_{GT} by model fitting. The network \mathcal{F}_θ parameterized by θ is designed to learn a mapping from the given sparse sampling data $\tilde{\mathcal{X}} \in \mathbb{R}^{W \times H \times S \times D_{Sparse}}$ to predicted multi-parameters \mathcal{Y}_{Pred} s.t. $\mathcal{Y}_{Pred} = \mathcal{F}_\theta(\tilde{\mathcal{X}}) \rightarrow \mathcal{Y}_{GT}$. We estimate multi-parametric scalar maps by minimizing the following cost function:

$$\min_{\theta} L_{Data}(\mathcal{F}_\theta(\tilde{\mathcal{X}}), \mathcal{Y}_{GT}) \quad (1)$$

where the first term is a data fidelity term used for penalizing the difference between the network output $\mathcal{F}_\theta(\tilde{\mathcal{X}})$ and ground truth \mathcal{Y}_{GT} .

2.2. Anatomical prior module

In clinical practice, different MR imaging settings will produce various multi-contrast images, which can provide complementary information to each other. This paper introduces an anatomical prior module as the additional regularization term for preserving structural details. Specifically, we extract T1w images using the hidden Markov random field model available in the 3D/4D+ imaging library in Python (DIPY)[21], categorizing voxels into three types of tissues: gray matter (GM), white matter (WM), and cerebrospinal fluid (CSF). This process generates tissue probability maps, as illustrated in Fig.1. It is noteworthy that each voxel’s probability value ranges from 0 to 1, representing the likelihood that the voxel belongs to the corresponding tissue type. For example, in the white matter probability map, a voxel’s value indicates its probability of being white matter.

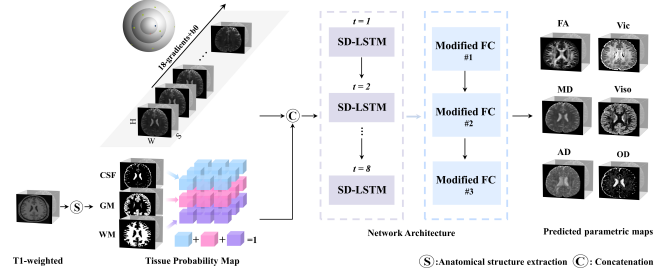


Fig. 1: An overview of the proposed framework. The input consists of two components: the upper branch with six DWIs and a b0 image, and the lower branch with tissue probability maps from T1w extraction. These inputs are concatenated and processed by the network to yield DTI and NODDI microstructural parameters, including fractional anisotropy(FA), mean diffusivity(MD), axial diffusivity(AD), intracellular volume fraction(Vic), isotropic volume fraction(Viso) and orientation dispersion index(OD).

2.3. Loss function

The objective function is defined based on the network output to enforce the consistency between the predicted \mathcal{Y}_{Pred} and the ground truth scalar maps \mathcal{Y}_{GT} obtained from the full sampling. Different from [15], our loss function is defined as:

$$\text{Loss} = \|\mathcal{Y}_{GT} - \mathcal{Y}_{Pred}\|_2^2 \quad (2)$$

where $\|\cdot\|_2^2$ denotes the squared L2 norm, used to compute the relative error between the predicted and ground truth values.

3. EXPERIMENTS

3.1. Dataset

This study employs preprocessed whole-brain diffusion MRI data from the publicly available Human Connectome Project (HCP) young adult dataset[22], acquired on a 3T MR scanner. A total of 111 subjects were randomly selected: 60 for training, 17 for validation, and 34 for testing. The diffusion MRI protocol consisted of three diffusion-weighted shells with b-values of 1000, 2000, and 3000 s/mm² respectively, and 90 directions per shell, along with eighteen reference (b = 0) volumes. Both DWI and T1w data were acquired at a spatical resolution of 1.25 mm isotropic. To prepare the training data, we use DMRITool[23] to select six uniformly distributed diffusion encoding directions per shell. Model fitting was primarily conducted using DIPY. Ground truth DTI metrics were obtained through tensor fitting of fully sampled diffusion data using a weighted least squares method as the reference gold standard. Ground truth NODDI metrics were derived using the AMICO[24] algorithm, also serving as gold standard references.

3.2. Experimental Settings

Our method was evaluated both qualitatively and quantitatively, and compared with traditional model fitting(MF) algorithms and deep learning-based methods, specifically including q_DL [7], 2D-CNN [11], and MESC-SD [12]. q_DL performed voxel-wise estimation using MLP without accounting for neighborhood information. 2D-CNN reshaped the raw data into slices and performed slice-wise estimation. MESC-SD considered the diffusion signals in a $3 \times 3 \times 3$

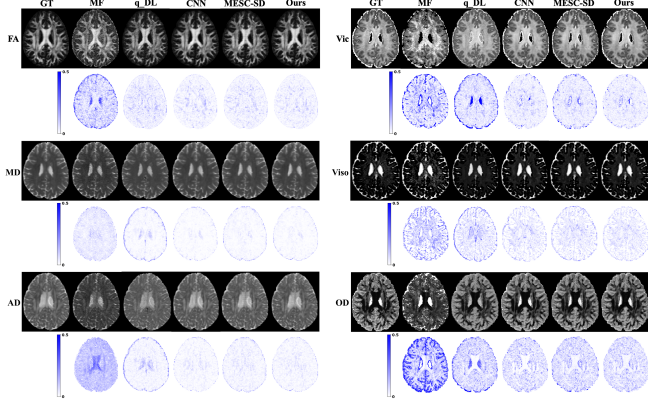


Fig. 2: The ground truth, estimated parametric maps and corresponding error maps based on MF, q_DL, CNN, MESC-SD, and Ours in a test subject with 6 diffusion directions per shell at b-values of 1000, 2000, and 3000 s/mm^2 .

image patch. We adopt MESC-SD as the backbone. To reduce memory consumption and training time, the inputs of our framework are matrices with $4 \times 4 \times 4$ patches in the spatial direction and diffusion-weighted signals in the angular direction, and the outputs are maps with $4 \times 4 \times 4$ in the spatial direction and eleven diffusion parameters in the angular direction, and then average the results for overlapping voxels. Performance was evaluated using Peak Signal-to-Noise Ratio (PSNR) and Structural Similarity Index (SSIM).

4. RESULTS

4.1. Comparison of state-of-the-art methods

Quantitative results are present in Table 1, demonstrating that the proposed method achieves better performance. Compared to the MESC-SD, the proposed method shows improvements over the baseline, validating its effectiveness in jointly estimating parametric maps. From the residual maps in Figure 2, it is evident that our method, incorporating the anatomical structure-guided module, successfully preserves fine-grained anatomical boundary details while effectively minimizing boundary noise.

4.2. Ablation Study: Comparison of Anatomical Priors

To evaluate the effectiveness of the anatomical structure extraction module, we compared two types of priors: the structural image prior and the anatomical structure prior. The results, presented in Table 2, demonstrate that both priors perform well, further underscoring the importance of anatomical data in guiding the extraction of DW signal features. Furthermore, the results in Table 2 indicate that the method equipped with the anatomical structure module outperforms its counterparts, further confirming the module’s effectiveness in filtering out anatomical boundary noise.

5. CONCLUSION

In this study, we propose an extendable framework for simultaneous estimation of parametric maps from multiple diffusion models using sparsely sampled q-space data. The proposed anatomical structure extraction module effectively guides DW signal feature extraction,

Table 1: The quantitative results were obtained with 6 diffusion directions per shell at b-values of 1000, 2000, and 3000 s/mm^2 . The best results are in bold.

Methods (18 DWIs)	PSNR						
	FA	MD	AD	Vic	Viso	OD	Average
MF	22.5003	28.2471	22.5526	18.6438	25.9331	18.6266	21.5238±0.5762
q_DL	29.9900	29.8063	29.0636	21.3592	26.6373	22.9165	25.2923±0.5505
CNN	33.8065	31.2779	30.6627	23.6787	29.3999	24.6650	27.4668±0.6532
MESC-SD	33.5589	31.5407	30.8925	24.1782	29.4174	25.1341	27.8358±0.6550
Ours	34.4223	32.1819	31.5219	28.7883	31.3110	27.8336	30.5126±0.5758
Methods (18 DWIs)	SSIM						
	FA	MD	AD	Vic	Viso	OD	Average
MF	0.8686	0.9577	0.9183	0.8735	0.9369	0.8492	0.9007±0.0114
q_DL	0.9418	0.9594	0.9471	0.9160	0.9336	0.9143	0.9354±0.0084
CNN	0.9664	0.9742	0.9674	0.9575	0.9598	0.9474	0.9621±0.0052
MESC-SD	0.9647	0.9728	0.9657	0.9563	0.9598	0.9494	0.9615±0.0053
Ours	0.9712	0.9753	0.9690	0.9776	0.9681	0.9680	0.9715±0.0041

Table 2: The quantitative comparison of PSNR and SSIM with different anatomical priors. The results were obtained with 6 diffusion directions per shell at b-values of 1000, 2000, and 3000 s/mm^2 .

Methods (18 DWIs)	PSNR						
	FA	MD	AD	Vic	Viso	OD	Average
DWIs	33.5589	31.5407	30.8925	24.1782	29.4174	25.1341	27.8358±0.6550
DWIs+T1w	34.0326	32.3151	31.6293	28.3280	31.0744	27.5306	30.2753±0.6023
DWIs+T1w tissue	34.4223	32.1813	31.5219	28.7883	31.3110	27.8336	30.5126±0.5758
Methods (18 DWIs)	SSIM						
	FA	MD	AD	Vic	Viso	OD	Average
DWIs	0.9647	0.9728	0.9657	0.9563	0.9598	0.9494	0.9615±0.0053
DWIs+T1w	0.9594	0.9731	0.9679	0.9755	0.9669	0.9657	0.9681±0.0136
DWIs+T1w tissue	0.9712	0.9753	0.9690	0.9776	0.9681	0.9680	0.9715±0.0041

filters out anatomical boundary noise, and achieves high-fidelity estimates with clearer tissue details. This flexible joint estimation framework leverages shared anatomical and diffusion information across multiple diffusion models to enhance estimation performance. Experimental results demonstrate that our method outperforms four state-of-the-art methods in both qualitative and quantitative evaluations. In future work, we aim to extend our approach to 5.0T brain imaging dataset [25] and a wider range of diffusion models.

6. COMPLIANCE WITH ETHICAL STANDARDS

This research study was conducted retrospectively using human subject data made available in open access by HCP[22]. Ethical approval was not required as confirmed by the license attached with the open access data.

7. ACKNOWLEDGMENTS

This research was partly supported by Shenzhen Medical Research Fund (No.B2402047), the National Natural Science Foundation of China (No.62222118, No.U22A2040), Shenzhen Science and Technology Program (No.RCYX20210706092104034, No.JCYJ20220531100213029), Key Laboratory for Magnetic Resonance and Multimodality Imaging of Guangdong Province (No.2023-B1212060052), and Youth Innovation Promotion Association CAS.

8. REFERENCES

- [1] Peter J Basser, James Mattiello, and Denis LeBihan, “MR diffusion tensor spectroscopy and imaging,” *Biophysical journal*, vol. 66, no. 1, pp. 259–267, 1994.
- [2] Ofer Pasternak, Sinead Kelly, Valerie J Sydnor, and Martha E Shenton, “Advances in microstructural diffusion neuroimaging

- for psychiatric disorders,” *Neuroimage*, vol. 182, pp. 259–282, 2018.
- [3] Hui Zhang, Torben Schneider, Claudia A Wheeler-Kingshott, and Daniel C Alexander, “NODDI: practical in vivo neurite orientation dispersion and density imaging of the human brain,” *Neuroimage*, vol. 61, no. 4, pp. 1000–1016, 2012.
 - [4] Yuxing Li, Zhizheng Zhuo, Chenghao Liu, Yunyun Duan, Yulu Shi, Tingting Wang, Runzhi Li, Yanli Wang, Jiwei Jiang, Jun Xu, et al., “Deep learning enables accurate brain tissue microstructure analysis based on clinically feasible diffusion magnetic resonance imaging,” *NeuroImage*, vol. 300, pp. 120858, 2024.
 - [5] Santiago Coelho, Jose M Pozo, Sune N Jespersen, Derek K Jones, and Alejandro F Frangi, “Resolving degeneracy in diffusion MRI biophysical model parameter estimation using double diffusion encoding,” *Magnetic resonance in medicine*, vol. 82, no. 1, pp. 395–410, 2019.
 - [6] Shanshan Wang, Ruoyou Wu, Sen Jia, Alou Diakite, Cheng Li, Qiegen Liu, Hairong Zheng, and Leslie Ying, “Knowledge-driven deep learning for fast MR imaging: Undersampled MR image reconstruction from supervised to un-supervised learning,” *Magnetic Resonance in Medicine*, vol. 92, no. 2, pp. 496–518, 2024.
 - [7] Vladimir Golkov, Alexey Dosovitskiy, Jonathan I Sperl, Marion I Menzel, Michael Czisch, Philipp Sämann, Thomas Brox, and Daniel Cremers, “Q-space deep learning: twelve-fold shorter and model-free diffusion MRI scans,” *IEEE transactions on medical imaging*, vol. 35, no. 5, pp. 1344–1351, 2016.
 - [8] Qiyuan Tian, Ziyu Li, Qiuyun Fan, Jonathan R Polimeni, Berkin Bilgic, David H Salat, and Susie Y Huang, “SDnDTI: Self-supervised deep learning-based denoising for diffusion tensor MRI,” *Neuroimage*, vol. 253, pp. 119033, 2022.
 - [9] Tobias Goodwin-Allcock, Ting Gong, Robert Gray, Parashkev Nachev, and Hui Zhang, “Patch-CNN: Training data-efficient deep learning for high-fidelity diffusion tensor estimation from minimal diffusion protocols,” *arXiv preprint arXiv:2307.01346*, 2023.
 - [10] Wenxin Fan, Jian Cheng, Cheng Li, Xinrui Ma, Jing Yang, Juan Zou, Ruoyou Wu, Qiegen Liu, and Shanshan Wang, “AID-DTI: Accelerating High-fidelity Diffusion Tensor Imaging with Detail-Preserving Model-based Deep Learning,” *arXiv preprint arXiv:2401.01693*, 2024.
 - [11] Eric K Gibbons, Kyler K Hodgson, Akshay S Chaudhari, Lorie G Richards, Jennifer J Majersik, Ganesh Adluru, and Edward VR DiBella, “Simultaneous NODDI and GFA parameter map generation from subsampled q-space imaging using deep learning,” *Magnetic resonance in medicine*, vol. 81, no. 4, pp. 2399–2411, 2019.
 - [12] Chuyang Ye, Xiuli Li, and Jingnan Chen, “A deep network for tissue microstructure estimation using modified LSTM units,” *Medical image analysis*, vol. 55, pp. 49–64, 2019.
 - [13] Taohui Xiao, Jian Cheng, Wenxin Fan, Jing Yang, Cheng Li, Enqing Dong, and Shanshan Wang, “RobNODDI: Robust NODDI Parameter Estimation with Adaptive Sampling under Continuous Representation,” *arXiv preprint arXiv:2408.01944*, 2024.
 - [14] SeyyedKazem HashemizadehKolowri, Rong-Rong Chen, Ganesh Adluru, and Edward VR DiBella, “Jointly estimating parametric maps of multiple diffusion models from under-sampled q-space data: a comparison of three deep learning approaches,” *Magnetic Resonance in Medicine*, vol. 87, no. 6, pp. 2957–2971, 2022.
 - [15] Wenxin Fan, Jian Cheng, Cheng Li, Xinrui Ma, Jing Yang, Juan Zou, Ruoyou Wu, Zan Chen, Yuanjing Feng, Hairong Zheng, et al., “DeepMpMRI: Tensor-decomposition Regularized Learning for Fast and High-Fidelity Multi-Parametric Microstructural MR Imaging,” *arXiv preprint arXiv:2405.03159*, 2024.
 - [16] Anastasia Yendiki, Manisha Aggarwal, Markus Axer, Amy FD Howard, Anne-Marie van Cappellen van Walsum, and Suzanne N Haber, “Post mortem mapping of connectonal anatomy for the validation of diffusion MRI,” *NeuroImage*, vol. 256, pp. 119146, 2022.
 - [17] Ruoyou Wu, Jian Cheng, Cheng Li, Juan Zou, Jing Yang, Wenxin Fan, Yong Liang, and Shanshan Wang, “CSR-dMRI: Continuous Super-Resolution of Diffusion MRI with Anatomical Structure-Assisted Implicit Neural Representation Learning,” in *International Workshop on Machine Learning in Medical Imaging*. Springer, 2024, pp. 114–123.
 - [18] Zan Chen, Chenxu Peng, Yongqiang Li, Qingrun Zeng, and Yuanjing Feng, “Super-resolved q-space learning of diffusion MRI,” *Medical Physics*, vol. 50, no. 12, pp. 7700–7713, 2023.
 - [19] Shijie Huang, Geng Chen, Kaicong Sun, Zhiming Cui, Xukun Zhang, Peng Xue, Xuan Zhang, He Zhang, and Dinggang Shen, “Super-resolution reconstruction of fetal brain MRI with prior anatomical knowledge,” in *International Conference on Information Processing in Medical Imaging*. Springer, 2023, pp. 428–441.
 - [20] Ziyu Li, Qiuyun Fan, Berkin Bilgic, Guangzhi Wang, Wenchuan Wu, Jonathan R Polimeni, Karla L Miller, Susie Y Huang, and Qiyuan Tian, “Diffusion MRI data analysis assisted by deep learning synthesized anatomical images (Deep-Anat),” *Medical image analysis*, vol. 86, pp. 102744, 2023.
 - [21] Eleftherios Garyfallidis, Matthew Brett, Bagrat Amirbekian, Ariel Rokem, Stefan Van Der Walt, Maxime Descoteaux, Ian Nimmo-Smith, and Dipy Contributors, “Dipy, a library for the analysis of diffusion MRI data,” *Frontiers in neuroinformatics*, vol. 8, pp. 8, 2014.
 - [22] David C Van Essen, Stephen M Smith, Deanna M Barch, Timothy EJ Behrens, Essa Yacoub, Kamil Ugurbil, Wu-Minn HCP Consortium, et al., “The WU-Minn human connectome project: an overview,” *Neuroimage*, vol. 80, pp. 62–79, 2013.
 - [23] Jian Cheng, Dinggang Shen, Pew-Thian Yap, and Peter J Basser, “Single-and multiple-shell uniform sampling schemes for diffusion MRI using spherical codes,” *IEEE transactions on medical imaging*, vol. 37, no. 1, pp. 185–199, 2017.
 - [24] Alessandro Daducci, Erick J Canales-Rodríguez, Hui Zhang, Tim B Dyrby, Daniel C Alexander, and Jean-Philippe Thiran, “Accelerated microstructure imaging via convex optimization (AMICO) from diffusion MRI data,” *Neuroimage*, vol. 105, pp. 32–44, 2015.
 - [25] Shanshan Wang, Shoujun Yu, Jian Cheng, Sen Jia, Changjun Tie, Jiayu Zhu, Haohao Peng, Yijing Dong, Jianzhong He, Fan Zhang, et al., “Diff5T: Benchmarking Human Brain Diffusion MRI with an Extensive 5.0 Tesla K-Space and Spatial Dataset,” *arXiv preprint arXiv:2412.06666*, 2024.